PHILOSOPHICAL MAGAZINE LETTERS
2021, VOL. 101, NO. 6, 232–241
https://doi.org/10.1080/09500839.2021.1909166

Gibbs energy minimisation model for the austenite-ferrite phase transformation in Fe-C-X-Y alloys

Alexandre Mathevon[a,b], Michel Perez[a,b], Véronique Massardier[a,b], Damien Fabrègue[a,b], Patrice Chantrenne[a,b] and Philippe Rocabois[a,b]

[a]Univ. Lyon – INSA Lyon – MATEIS – UMR CNRS 5510, Villeurbanne, France; [b]Fives Keods, Maisons-Alfort, France

ABSTRACT

A new model has been developed to predict austenite ↔ ferrite transformation kinetics in steels. For each alloying element, the concentration profile is computed solving a *unique* diffusion equation (including the 2 phases and the interface). The interface is described assuming linear variation of chemical potentials, saving thus computational time. Interface motion is driven by the minimisation of Gibbs energy. The model naturally reproduces the transition between thermodynamic equilibria (Para equilibrium, Local equilibrium with negligible partitioning, Local equilibrium) during heating. The validity of the model for reverse transformation has been validated on ternary and quaternary systems Fe-C-(Mn-Si-Mo) on decarburisation experiments.

ARTICLE HISTORY
Received 16 January 2020
Accepted 22 March 2021

KEYWORDS
Modeling; thermodynamics; phase transformation kinetics; steels; Gibbs energy minimisation

2010 MATHEMATICS SUBJECT CLASSIFICATION
74N25

1. Introduction

The development of steel grades such as Dual-Phase, Transformation Induced Plasticity [1] or Medium Manganese [2] steels is based on a thorough knowledge of phenomena occurring during austenite (γ) ↔ ferrite (α) phase transformations. These phenomena (namely recrystallisation, recovery, nucleation, diffusion/interface controlled growth), may occur simultaneously and interact with each other, leading to complex overall transformation kinetics.

Several types of modelling approaches have been proposed in order to understand the role of alloying elements (C, N, Mn, Ni, Cr, Si,…). The simplest view is based on the concept of a sharp interface between ferrite and austenite, where some kind of thermodynamical equilibrium is fulfiled (i.e. Paraequilibrium, local equilibrium with or without partitioning – see ref. [3] for more details). Thermocalc diffusion module (DICTRA) is based on these assumptions [4] and the equilibrium conditions are obtained using CALPHAD methods. Unfortunately, this approach cannot reproduce kinetics that deviate

CONTACT Alexandre Mathevon alexandre.mathevon@insa-lyon.fr

from these equilibrium (i.e. transition from para to local equilibrium) and solute flux balance at the interface often leads to numerical issues [5].

Mixed-mode models overcome the problem of solving complex multiple elements diffusion profiles by introducing the concept of interface mobility, with its own kinetics. This approach makes it possible to reproduce experimental kinetics [6–10], but the mobility applied to take into account the interaction of other elements has no physical meaning, limiting thus predictive capacities of such models.

Another family of models assume a quasi-permanent regime at the interface, where the transformation kinetics is driven by the balance between energy dissipation and driving force [11,12]. However, these models hardly capture changes in interface direction due to manganese partitioning while having a complete monitoring of the concentration profiles within the 2 phases.

Chen and Perevoshchikova [13,14] proposed a complete 2D-Phase Field (PF) model to describe the austenite formation during a heating within a ferrite-pearlite matrix. This study is based on a Mixed-mode model including solute drag to take into account the slow partitioning of the substitutional elements. The PF approach is nevertheless based on a mathematical approach that aims to smooth interface and interpolate the properties of each phase within the interface, posing the problem of the real *vs* modelled interface characteristic size.

In this paper, a new algorithm has been developed to predict $\gamma \leftrightarrow \alpha$ transformation kinetics in complex systems iron alloys. The originality of this approach is that, for each element, the concentration profile is computed solving a *unique* diffusion equation (including the 2 phases and the interface), instead of solving diffusion equations in each phase and dealing with the mass conservation equations of each species to get the interface velocity. The interface is described using chemical potentials driving the thermodynamics of the system. Interface motion and solute fluxes are treated in a simple framework, allowing to predict the kinetics of phase transformations in many cases without any fitting parameters.

2. Simulation method

The model described in this paper is based on the prediction of (i) concentration profiles for all elements in ferrite and austenite, and (ii) interface migration, thanks to the minimisation of the total Gibbs energy in the entire system (i.e. 1D phase field approach).

The local Gibbs energy of a given phase is the weighted sum of the partial molar Gibbs energies (chemical potentials) of each element, given by Gibbs-Duhem relation. For the sake of computational time, it is assumed here that the energy of a multi-component system (e.g. FeXY) is the linear combination of the energy of binary systems (FeX+FeY) composing the multi-component system. This hypothesis leads to the following expression for the Gibbs energy for node i:

$$G|_i = \mu^0_{\mathrm{Fe},j} + \sum_k [\mu^B_{\mathrm{Fe},j}(X_k|_i) \cdot (1 - X_k|_i) + \mu^B_{k,j}(X_k|_i) \cdot X_k|_i - \mu^0_{\mathrm{Fe},j}] \tag{1}$$

where $\mu^0_{\mathrm{Fe},j}$ is the chemical potential of pure iron in phase j, $\mu^B_{\mathrm{Fe},j}(X_k)$ and $\mu^B_{k,j}(X_k)$ are the chemical potentials of iron and element k in a binary Fe/k system of composition $X_k|_i$ in phase j (α or γ).

With such an approach, the energy of a multi-component system containing n elements only requires the knowledge of n binary databases, that can be calculated from TCFE8 Thermocalc database *a priori*. In other words, cross interaction terms are neglected with such a linear assumption.

A validation test was carried out to compare the use of Gibbs-Duhem equation (using TQ interface and TCFE8 database) instead of Equation (1). It led to less than 3% error on the phase fractions at the final equilibrium for a $0.17\mathrm{C} - 1.7\mathrm{Mn}$ steel at 780 °C. Despite providing exact fractions predicted by TCFE8 database, the complete coupling (Gibbs-Duhem equation and TQ interface) suffers from intractable computational times. This is why we use Equation (1) to previously generate a database from TCFE8.

These conditions are valid in all applications presented hereafter because they are limited to rather low-alloy compositions. For more concentrated alloys, an additional terms should be considered. Moreover, taking into account the interfacial energy for 2D or 3D simulations as well as additional physical phenomena (strain transformation, electromigration,…) affecting the Gibbs energy could be straighforwardly added to the model. The weighted sum of the Gibbs energies over all nodes gives the total energy of the system, which will be the potential function, that will be minimised when considering interface motion.

Chen et al. [12] uses a modified Fick equation to model diffusion profiles within a mobile interface with chemical potential gradients. The diffusion equation providing the concentration profiles of each chemical element k in 1D is extended to the whole system in a fixed reference which leads to:

$$\frac{\partial}{\partial x}\left(D_{k,j}\frac{\partial C_k}{\partial x} + \frac{C_k D_{k,j}}{RT}\frac{\partial \mu^0_{k,j}}{\partial x}\right) = \frac{\partial C_k}{\partial t} \tag{2}$$

where C_k is the concentration of element k, T is the temperature, x is the distance, R is the ideal gas constant, $D_{k,j}$ is the diffusion coefficient and $\mu^0_{k,j}$ is standard chemical potential for pure iron of element k in phase j (as shown in Figure 1 b). Boundary conditions fulfil:

$$\left.\frac{\partial C_k}{\partial x}\right|_{x=0,L} = 0 \text{ (closed)} \quad \text{or} \quad C_k|_{x=0,L} = C_0 \text{ (open)} \tag{3}$$

whether the system is closed or open (C_0 is the imposed concentration at sample boundaries).

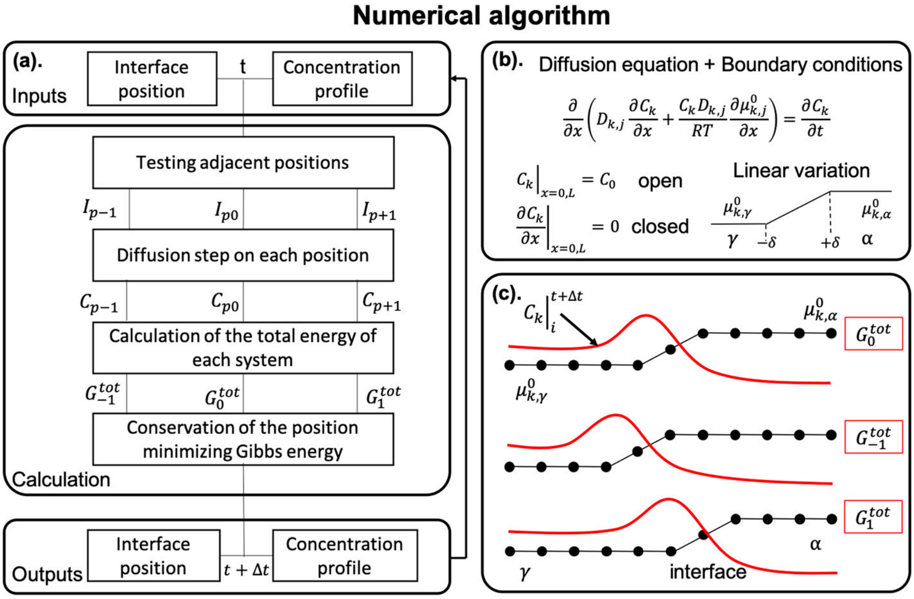

Figure 1. (a) GEM model algorithm. (b) Diagram of linear chemical potential profile used. (c) Example of concentration profile obtained when selecting the interface position.

Equation (2) is equivalent to the classical Fick's law outside the interface ($\partial\mu^0_{k,j}/\partial x = 0$), where concentration gradients tend to flatten. Within the interface of size 2δ, the chemical potential is supposed to vary linearly between the chemical potential of ferrite ($\mu^0_{k,\alpha}$) and austenite ($\mu^0_{k,\gamma}$) (see Figure 1b) in order to solve diffusion equations in a unique framework. Compared to Ref. [12], velocity does not appear explicitely in Equation (2) because we use a Eulerian specification (fixed integration gird), whereas Chen et al. used a Lagrangian specification (following the interface). Note that it is possible to add a potential well at the interface in GEM model, in agreement with Cahn that may lead to an increase of solute atoms segregating and interface friction. The diffusion coefficient of element M inside the interface D_M^{Int} is assumed to be the geometric average of the diffusion coefficient of M in austenite D_M^{γ}, ferrite D_M^{α} and the ferrite grain boundary D_M^{GB}. Value of D_M^{GB} are obtained from [15].

The diffusion equation (Equation (2)) is solved using 1D implicit scheme for each element k. We choose for each node i the following discretised equation:

$$\begin{aligned}\frac{C_k|_i^{t+\Delta t}-C_k|_i^t}{\Delta t}\\ =\frac{D_{k,j}|_i(C_k|_{i+1}^{t+\Delta t}-C_k|_i^{t+\Delta t})+D_{k,j}|_{i-1}(C_k|_{i-1}^{t+\Delta t}-C_k|_i^{t+\Delta t})}{\Delta x^2}\\ +\frac{D_{k,j}|_{i+1}C_k|_{i+1}^{t+\Delta t}(\mu^0_{k,j}|_{i+1}-\mu^0_{k,j}|_i)-D_{k,j}|_i C_k|_i^{t+\Delta t}(\mu^0_{k,j}|_i-\mu^0_{k,j}|_{i-1})}{RT\Delta x^2}\end{aligned} \tag{4}$$

The interface displacement is based on total Gibbs Energy Minimisation (GEM) with respect to the interface position:

$$\frac{\partial G^{tot}}{\partial x_{\text{int}}} = 0 \text{ with } G^{tot} = \sum_i G|_i \tag{5}$$

where x_{int} is the interface position. The general algorithm used in this approach is shown in Figure 1 a. At each time step, (i) the total Gibbs energy of the system is calculated after a diffusion step (energy G_0^{tot}); then, (ii) the interface is moved by one grid step forward and a diffusion step is performed (energy G_{+1}^{tot}); finally, (iii) the interface is moved by one grid step backward and a diffusion step is performed (energy G_{-1}^{tot}). The position of interface corresponds to the position of the lowest total Gibbs energy (G_{-1}^{tot}, G_0^{tot} or G_{+1}^{tot}). At each calculation step, the time and space steps is the same for all chemical elements and with a fixed space step through the simulation small enough to ensure a negligible interface size compare to system size. Time steps have been optimised in order (i) to obtain an accurate interface velocity and (ii) to optimise computation time. For a given interface velocity v (fixed by the physics of the system), the displacement Δd of the interface in one time step Δt is given by $\Delta d = v\Delta t$. If $\Delta d \ll \Delta x$ (Δx is the space step), the time step can be increased in order to save computation time. If $\Delta d \gg \Delta x$, probing only adjacent positions (G_{tot}^{-1}, G_{tot}^{0} and G_{tot}^{+1}) is not enough and would lead to incorrect interface velocity, time step has therefore to be decreased. The ideal situation is then $\Delta d \lesssim \Delta x$. Practically, this ideal scheme is ensured by increasing the time step if the system lies more than 5 time steps at the same position and decreasing the time step if the system lies less than 3 time steps at the same position. Finally, the width of the interface has negligible effect on the transformation kinetics (in a range tested from 0.5 nm to 50 nm according to the literature) if it remains less than 5% of the total length of the system.

3. Results and discussion

The relevance of this model, is first tested on the ferrite to austenite transformation during an isothermal treatment of a Fe–0.17 C–1.7Mn low-alloy steel.

During heating of pearlitic Fe-C-Mn steel, Wei et al. [16] and Chantrenne et al. [5] showed that the austenite formation kinetics occurs in 4 stages to reach final ortho-equilibrium (see Figure 2 a). In the present study, the initial structure is a mixture of deformed ferrite and pearlite resulting from hot and cold rolling (see Ref. [17] for more details). The transformation was modelled by a 5 μ m 1D simulation cell (10000 nodes and $\delta = 5$ nm) with closed boundary conditions for each elements, corresponding to half the distance between the Mn rich segregation bands. Diffusion coefficients from the MOBFE3 mobility database were used and summarised in Table 1.

The simulation starts with a 0.1 μm austenite region (containing 6.67 wt%C and 10 wt%Mn), resulting from the fast transformation of cementite (see Ref. [5,10] for more details on this initial state).

Figure 2a shows the ferrite to austenite transformation kinetics during isothermal treatments performed at 760 °C and 780 °C resulting from GEM model. The transformation occurs in 4 stages. The transformation is controlled by (I) C diffusion without Mn diffusion (i.e. para-equilibrium), (II) Mn diffusion in ferrite (i.e. local equilibrium without partioning), (III) Mn diffusion in austenite, (IV) Mn diffusion in ferrite (i.e. ortho-equilibrium). The back and forth interface motion observed in Figure 2a is due to the initial high Mn concentration of cementite, that needs to redistribute along the whole sample before reaching full equilibrium (see diffusion profiles in

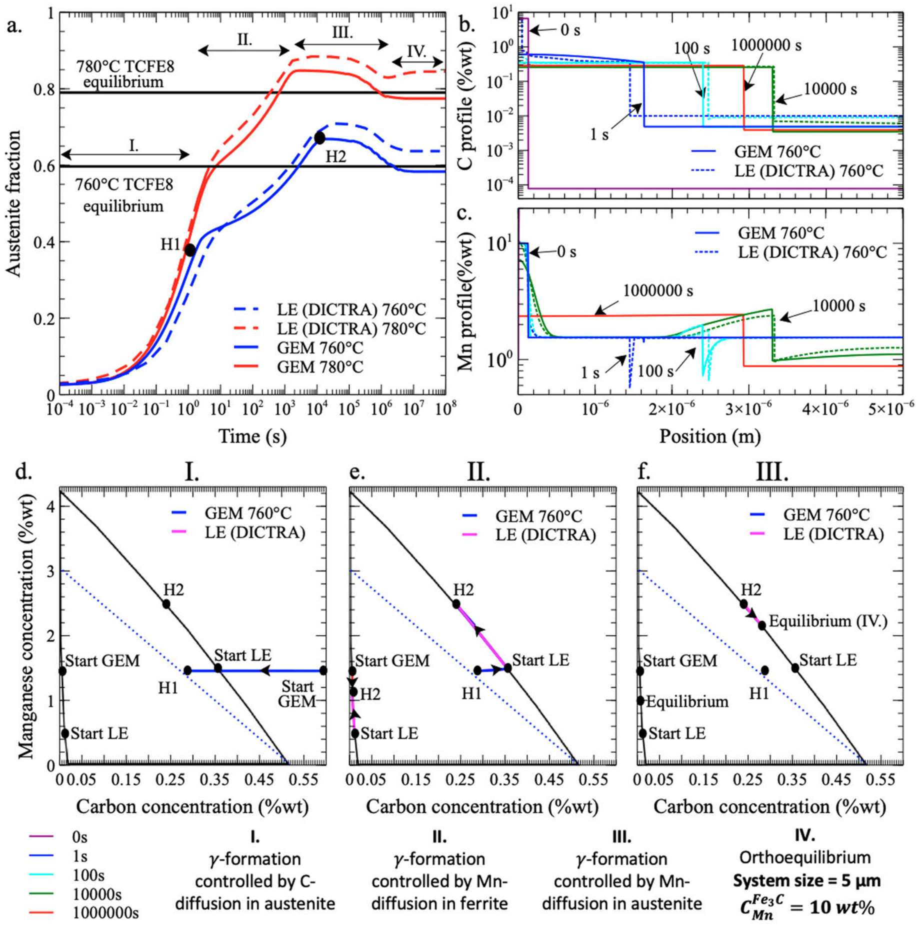

Figure 2. (a) Comparison of austenitic transformation kinetics between LE model (DICTRA), Thermocalc TCFE8 equilibrium and GEM model. (b) Carbon and (c) manganese concentration profile snapshots at 760 °C. Transition trajectories of compositions at the interface on the isothermal section of the Fe-C-Mn phase diagram at 760 °C for phase transformations in stage: d) I. ,e) II. and f) III.

Figure 2 b,c). The first stage of the transformation is driven by the carbon diffusion in austenite leading to concentrations close to the one predicted by the para-equilibrium (no Mn diffusion, see Figure 2 d), in contrast to DICTRA, which imposes local equilibrium at the interface. Subsequently, the system reaches an equilibrium state (with manganese diffusion in ferrite) close to local equilibrium without partitioning. Then, the system reaches local equilibrium at the interface and finally ortho-equilibrium (see Figure 2 e,f).

Transformation kinetics from GEM model are compared with simulations resulting from LE (DICTRA). Both approaches lead to similar results. As stated in Ref. [5], DICTRA does not respect mass balance, explaining thus the 5% final austenite fraction difference between DICTRA and LE equilibrium for long simulation times. GEM respects mass balance but leads to a 2% error due to the use of simplified Equation (1) (linear combination of binary systems).

This example illustrates the capability of GEM model to move the interface from one way to the other without any modification of the code. Moreover, the GEM model only needs initial concentration fields in both phases without any additional assumption on the type of equilibrium: i.e. the transition between different kinds of equilibrium (para → local → full) is naturally described. The model also conserves alloying element mass throughout the simulation. In addition, for the same simulation system, the GEM model allows to divide the calculation time by 60 compared to DICTRA and a factor 50 compared to another implementation of LE model [5]. This time reduction is mainly due to the choice of this model on the interface description. Indeed, at each time step the GEM model has only three profiles to compute, whereas the DICTRA algorithm is based on a loop that finds the interface velocity satisfying local equilibrium and mass balance. This optimisation is all the more complex when the number of elements increases.

In a second step, decarburisation experiments are a smart way of studying austenite to ferrite transformation because it overpasses many difficulties encountered in more ‘classical’, so called precipitation transformations (e.g. nucleation, overlap of carbon diffusion fields). In addition, the literature includes numerous accurate results on Fe-C-X and Fe-C-X-Y systems: i.e. the displacement of the interface is measured with a precision of approximately 5 μm over distances of about 300 μm [11,18–20]. Note that these

Table 1. Activation energy (Q) and pre-exponential factor (D_0) of diffusion coefficients of C and Mn in ferrite and austenite used for austenite formation (extracted from the MOBFE3 database of Thermo-Calc).

Elements	C in α	C in γ	Mn in α	Mn in γ
Q (kJ/mol)	115.8	144.2	321.8	263.2
D_0 (m^2/s)	9.9×10^{-5}	1.7×10^{-5}	4.6	1.7×10^{-5}

decarburisation experiments involve temperatures close to AC1 and transformation kinetics ten times slower than precipitation transformations.

Initial simulation boxes for decarburisation are semi-infinite 1D (500 µm, 100000 nodes and $\delta = 50\,\mathrm{nm}$) with homogeneous nominal composition of the steel. Simulation starts with one node of ferrite, for which the C concentration is forced to be 0, at one extremity of the simulation cell. The other extremity has a zero flux condition. The carbon diffusion coefficient in austenite and ferrite (dependent on carbon content) was obtained from [21,22].

Figure 3 compares GEM model with experiments for 2 ternary and 2 quaternary alloys. Without any fitting parameter, the agreement is remarkable for all systems. For the sake of comparison, interface position under Local equilibrium with negligible partitionning and paraequilibrium are represented in Figure 3. These equilibrium conditions are rarely satisfied in real systems. The self consistent model of Zurob et al. [11] based on Gibbs Energy balance between interface friction and driving force is also compared to experiments and GEM model. It can be observed on Figure 3 that GEM and Zurob's models are superimposed for all cases, except for the the quaternary Fe-C-Mn-Si system, where Zurob's model fails to describe experimental results with the same parameters as those adjusted on ternary systems.

Note that solute drag, that underlies the GEM model and the self consistent model of Zurob (as well as the GEB model of Chen et al. [12]) is responsible for monitoring phase-transformation kinetics. We also have tested the GEM model with the same potential well as Zurob and GEB models, without any significant effect on both transformation kinetics which establishes that the potential well is not a necessary ingredient of GEM model. Moreover, this transformation slowdown has been observed in the GEM model for ferrite precipitation simulations at lower temperatures (higher driving forces and higher transformation kinetics). In these conditions, the introduction of a potential well leads to solute atoms segregation at the interface that hinders interface motion and leads to a drastic slowdown of the interface motion.

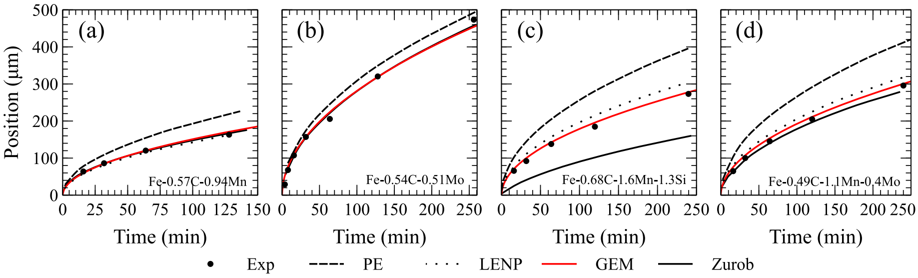

Figure 3. Decarburisation kinetics for (a) Fe-0.57C-0.94Mn (806 °C) (b) Fe-0.54C-0.51Mo (806 °C) (c) Fe-0.68C-1.58Mn-1.33Si (806 °C) (d) Fe-0.49C-1.09Mn-0.42Mo (806 °C). The results of the Zurob model presented were extracted from [11,18,19]

We have presented a new phase transformation model based on the Minimisation of Gibbs Energy (GEM model). As entry parameters, it requires diffusion coefficients of all elements, as well as a thermodynamic database, that can eventually be created *a priori*, from linear combination of binary systems, computed from TCFE8 database. GEM model provides the kinetics of $\alpha \rightarrow \gamma$ and $\gamma \rightarrow \alpha$ transformations without imposing any type equilibrium conditions at the interface. GEM model accurately reproduces transformation kinetics and concentration profiles for all solute species (including C) for heating and cooling. GEM model is also able to account for solute drag that slows down interface motion, but introducing a chemical potential well at the interface is not a necessary ingredient to correctly describe decarburisation experiments. This numerical approach respect mass balance and leads to drastic reduction of the computation time compared to existing models. Extension to systems containing more than 4 elements is relatively simple. Cementite dissolution as well as non-isothermal conditions could also be relatively straightforwardly implemented.

Acknowledgments

S. van der Zwaag and H. Farahani are gratefully acknowledged for stimulating discussions, detailed explanations of GEB model and warm exchanges.

Disclosure statement

No potential conflict of interest was reported by the author(s).

Notes on contributors

Alexandre Mathevon received his PhD degree from Institut National of Applied Sciences of Lyon in 2020. His research interests include the characterisation and modelling of microstructural evolutions and their links with mechanical properties in steel.

Michel Perez received the PhD degree in 2000 from Grenoble Institute of Technology, France. He was appointed Assistant Professor (2001), Associate Professor (2007) and full Professor (2010) at INSA Lyon, France. His research interests include the characterisation and modelling of precipitation and allotropic phase transformations in various metallic alloys. He has also been developing simulations at the atomic scale to better understand structural properties of various materials: polymers, elastomers, ceramics and metals.

Véronique Massardier received his PhD degree from Institut National of Applied Sciences of Lyon in 1994. She is an assistant professor in the Metals and Alloys team of the MATEIS laboratory where she studies the relation between the microstructure and the mechanical properties of metals (steels, aluminium allloys, composites…).

Damien Fabrègue received hiq PhD degree from Institut National Polytechnique de Grenoble in 2004. He has been appointed as associate professor in 2006 in the National Institute of Applied Science in Lyon in 2006. His research interest concerns the link between the thermo-mechanical processing, the microstructure and the resultant mechanical properties.

Patrice Chantrenne received his Ph.D. degree in 1995 from INSA de Lyon. His is now Professor in MATEIS laboratory at INSA de Lyon. His research interests concern heat and mass transfer with a multiscale analysis (from atomic to usual scales). In metallurgy, he focuses on the influence of the thermal treatments on final microstructure of the matter, especially when thermal treatment is induced by an electric field.

References

[1] D. K. Matlock, P. J. Gibbs, J. G. Speer and E. D. Moor JESTECH 15 (2012) p.1.
[2] Y.-K. Lee and J. Han, Mater. Sci. Tech. 31 (2014) p.843.
[3] M. Goune, F. Danoix, J. Agren, Y. Bréchet, C. Hutchinson, M. Militzer, G. Purdy, S.V.D. Zwaag and H. Zurob, Mater. Sci. Eng. R. 92 (2015) p.1.
[4] J.O. Andersson, T. Helander, L. Hoglund, P.F. Shi and B. Sundman, Calphad 26 (2002) p.273.
[5] P. Chantrenne, M. Perez, M. Ollat, V. Massardier, D. Fabregue and R. Philippe, Model. Simul. Mater. Sci. Eng. 27 (2019) p.065007.
[6] G.P. Krielaart, J. Sietsma and S.V.D. Zwaag, Mater. Sci. Eng. 237 (1997) p.216.
[7] J. Sietsma and S. van der Zwaag, Acta Mater. 52 (2004) p.4143.
[8] C. Bos and J. Sietsma, Scripta Mater. 57 (2007) p.1085.
[9] C. Bos and J. Sietsma, Acta Mater. 57 (2009) p.136.
[10] M. Ollat, M. Militzer, V. Massardier, D. Fabregue, E. Buscarlet, F. Keovilay and M. Perez, Comput. Mater. Sci. 149 (2018) p.282.
[11] H.S. Zurob, D. Panahi, C.R. Hutchinson, Y. Brechet and G.R. Purdy, Metall. Mater. Trans. A 44 (2012) p.3456.
[12] H. Chen and S.V.D. Zwaag, Acta Mater. 72 (2014) p.1.
[13] H. Chen, B. Zhu and M. Militzer, Metal. Mater. Trans. A 47 (2016) p.3373.
[14] N. Perevoshchikova, B. Appolaire, J. Teixeira, E. Aeby-gautier and S. Denis, Comput. Mater. Sci. 82 (2014) p.151.
[15] J. Fridberg, L.E. Törndahl and M. Hillert, Jernkontorets Ann 153 (1969) p.263.
[16] R. Wei, M. Enomoto, R. Hadian, H.S. Zurob and G.R. Purdy, Acta Mater. 61 (2013) p.697.
[17] M. Ollat, V. Massardier, D. Fabregue, F. Keovilay, E. Buscarlet and M. Perez, Metal. Mater. Trans.A (2017) p.1.
[18] C. Qiu, H.S. Zurob and C.R. Hutchinson, Acta Mater. 100 (2015) p.333.
[19] W.W. Sun, H.S. Zurob and C.R. Hutchinson, Acta Mater. 139 (2017) p.62.
[20] D. Panahi, H. Van Landeghem, C.R. Hutchinson, G. Purdy and H.S. Zurob, Acta Mater 86 (2015) p.286.
[21] J. Ågren, Acta Metal. 30 (1982) p.841.
[22] J. Ågren, Scripta Metal. 20 (1986) p.1507.